JOM, Vol. 75, No. 11, 2023
https://doi.org/10.1007/s11837-023-06023-x

Structural Phase Stability Analysis on Shock Wave Recovered Single- and Polycrystalline Samples of $NiSO_4.6H_2O$

A. SIVAKUMAR,[1,10] S. SAHAYA JUDE DHAS,[2] LIDONG DAI,[1,11] P. SIVAPRAKASH,[3] T. VASANTHI,[4] V.N. VIJAYAKUMAR,[5] RAJU SURESH KUMAR,[6] V. PUSHPANATHAN,[7] S. ARUMUGAM,[8] IKHYUN KIM,[3,12] and S.A. MARTIN BRITTO DHAS[9,13]

1.—Key Laboratory of High-temperature and High-pressure Study of the Earth's Interior, Institute of Geochemistry, Chinese Academy of Sciences, Guiyang 550081, Guizhou, China. 2.—Department of Physics, Kings Engineering College, Sriperumbudur, Chennai, Tamilnadu 602 117, India. 3.—Department of Mechanical Engineering, Keimyung University, Daegu 42601, Republic of Korea. 4.—Departmet of Physics, PPG Institute of Technology, Coimbatore, Tamil Nadu 641 035, India. 5.—Department of Physics, Condensed Matter Research Laboratory, Bannari Amman Institute of Technology, Sathyamangalam, Tamil Nadu 638 401, India. 6.—Department of Chemistry, College of Science, King Saud University, P.O. Box 2455, 11451 Riyadh, Saudi Arabia. 7.—Department of Chemistry, Dr. M.G.R. Government Arts and Science College for Women, Villupuram, Tamil Nadu 605 602, India. 8.—Centre for High Pressure Research, School of Physics, Bharathidasan University, Tiruchirapalli, Tamilnadu 620 024, India. 9.—Shock Wave Research Laboratory, Department of Physics, Abdul Kalam Research Center, Sacred Heart College, Tirupattur, Tamil Nadu 635 601, India. 10.—e-mail: shivushock777@gmail.com. 11.—e-mail: dailidong@vip.gyig.ac.cn. 12.—e-mail: kimih@kmu.ac.kr. 13.—e-mail: martinbritto@shctpt.edu

Analysis of materials' stability based on the crystallographic structure by the enforced external impulsion of dynamic shock waves is now considered one of the most currently required investigations from the perspective of academic and technological sciences. While performing shock wave experiments on single- and polycrystalline materials, the results obtained are abrupt, so there is no a clear understanding of the changes occurring. In this context, the authors have demonstrated the crystallographic structural stability of polycrystal nickel sulfate-hexahydrate (NSH) [$NiSO_4.6H_2O$] under dynamic shock wave-exposed conditions, comparing the results to the previously reported single-crystal $NiSO_4.6H_2O$. The shock wave impact on the titled polycrystalline samples has been assessed by Raman spectroscopy, X-ray diffraction, electronic spectral and magnetic properties. Based on the observed results, the test samples do not undergo any crystallographic structural transitions even at 100 shock pulses-loaded conditions, whereas the single crystal $NiSO_4.6H_2O$ undergoes continuous phase transitions between the crystalline and amorphous states against the shock pulses of counts 1 to 8. Based on the systematic investigations of the obtained results, it is authenticated that the polycrystalline samples have higher structural stability than the single crystalline samples of $NiSO_4.6H_2O$.

INTRODUCTION

Investigation of the sustainability of the crystallographic structure of materials under extreme environmental conditions such as shock waves, temperature, pressure, and high energy rays (gamma rays, X-rays, etc.) is considered as one of the fundamental research topics in every aspect of

(Received March 15, 2023; accepted July 18, 2023; published online August 15, 2023)

the materials science branches, and it is still one of the most attractive research topics sought after to determine a convincing relationship between the crystallographic phase and its stability regarding their functional properties.[1–4] Note that single and polycrystalline samples show drastic changes in their functional properties as well as their structural stability.[5–8] As only a few publications are available on the topic of the sustainability of the crystallographic structure of single and polycrystalline samples under extreme environmental conditions, it is worthwhile to fill the gap with the exploration of the results of the stability of a few materials under shocked conditions. Along those lines, investigating the crystallographic structural stability of polycrystal $NiSO_4.6H_2O$ under shocked conditions could be a step forward because, considering the industrial applications, stability of the structure-property profiles is highly necessary to avoid damage to the devices while under exposure to highly fluctuating temperatures and pressure.[9,10] It is well known that polycrystalline materials have higher structural stability than single-crystalline materials under external stimuli whereas in the case of polycrystalline samples, the internal grain boundaries and grain-grain interfaces could resist any kind of phase transitions.[5–8]

The shock tube is one of the simple and efficient devices capable of providing the scope to make an effective assessment of the crystallographic and mechanical stability of materials including size-dependent materials such that it can be used instead of high-cost static high-pressure compression techniques such as diamond anvil cells (DACs). In recent years, research on the impact of shock waves on materials has been increasing linearly because of its capability to provide outstanding results including that of size-dependent materials.[11–15] While shock waves are loaded on a sample, they might experience four types of changes broadly from a crystallographic point of view such that they may undergo (1) crystalline to crystalline phase transition,[14] (2) crystalline to amorphous phase transition and vice versa,[16–18] (3) a few lattice deformations and defects without any kind of phase transitions,[19,20] and (4) neither phase transitions nor lattice deformations.[4,10] Note that the shock wave impact on materials varies significantly while performing the experiment on poly- and single-crystalline samples (micro- and nanopowder). The quantum of the present work is necessitated by the list of a few reports on the impact of shock waves on optically transparent single- and polycrystalline (microparticles) samples while loaded with dynamic shock pulses. The single crystals featured in the reports are ammonium dihydrogen phosphate,[21] ammonium pentaborate hexahydrate,[22] potassium sulfate,[23] nickel sulfate hexahydrate,[24] and potassium acid phthalate.[25] The micro-sized particles featured are ammonium dihydrogen phosphate,[26] potassium dihydrogen phosphate,[27] xylenol-doped potassium dihydrogen phosphate,[28] vanadium,[29] and magnesium diboride.[30] Among the above-mentioned single-crystal reports, potassium sulfate undergoes switchable structural transitions in accordance with the applied counts of shock pulses,[23] but in the case of polycrystalline samples, no such phase transition is observed.[31] Under dynamic shock wave-exposed conditions, nickel sulfate hexahydrate crystal experiences the reversible phase transition of crystalline to amorphous phase transition in accordance with the exposed shock pulses.[24] In the present scenario, it is intended to analyze the outcomes of the polycrystalline samples of nickel sulfate hexahydrate under dynamic shock wave-exposed conditions such that understanding of the shock resistance behavior of single- and polycrystalline samples could be a reality because the titled material of nickel sulfate hexahydrate (NSH) is one of the promising materials for the band-pass filters, frequency converters, and signal processing applications.[32,33] Many researchers have examined the properties of NSH crystal regarding the crystal growth aspect[34,35] and thermodynamic perspective.[36] Note that the test crystal can be crystallized in two different crystal structures, which are the $P4_12_12$ space group (α-phase) with the tetragonal crystal structure at ambient conditions and the C_2/C space group (β-phase) with the monoclinic crystal structure at 58 °C, and un-hydrated nickel sulfate crystal can be produced at 180 °C.[34–36] During the dehydration process, the sequence of changes has been $6H_2O$ to $4H_2O$ and $4H_2O$ to H_2O and finally to un-hydrated $NiSO_4$.[36] In this work, the stability of the crystallographic phase for the polycrystalline NSH crystals is presented and demonstrated under shock-exposed conditions such that the observed data have been evaluated by XRD, Raman and UV-DRS spectroscopy. Surprisingly from the obtained results, the polycrystalline NSH crystals have been identified as not having undergone any of the above-mentioned phase transitions such that it retains the crystallographic phase even if it is at 100 shocked conditions of 2.2 Mach number.

EXPERIMENTAL SECTION

The single-crystal growth details of the title material[32] and dynamic shock wave exposing procedure (Fig. S1)[37] have been discussed in the previous report and are also provided in the supplementary section. For this study, three fine powder samples of $NiSO_4.6H_2O$ crystals have been chosen, of which one sample has been kept as the pristine sample and the rest used for the shock wave loading of 50 and 100 shock pulses. One shock pulse has a transient pressure and temperature of 2.0 MPa and 864 K, respectively. Subsequently, 50 and 100 shock pulses have been loaded on the respective samples, and thereafter the required analytical studies have been undertaken for the

pristine and shocked samples such that the results of the single and polycrystalline samples could be compared.

Analytical Characterization Details

The details of analytical instruments that have been utilized for the required characterizations are to be described. Powder X-ray diffraction (PXRD) [Rigaku – Smart Lab X-Ray Diffractometer, Japan, $CuK\alpha_1$ as the X-ray source (λ = 1.5407 Å), with step precision of ± 0.001°] has been used. A Renishaw model Raman spectrometer with laser line of 532 nm and power 50 mW has been utilized such that the Raman instrumental observation has been carried out using the pelletized form of samples. An ultra-violet diffused reflectance spectroscope (UV-DRS- ShimadzuUV-3600 plus) and a vibrating sample magnetometer (Lake Shore, Cryotronics) have been utilized to understand the structural and magnetic structural stability of the test samples under shocked conditions.

RESULTS AND DISCUSSION

XRD Analysis

In the process of the current experimental search, powder X-ray diffractometry has been taken up in such a way that the crystallographic phase stability could be assessed for the polycrystalline samples. The XRD patterns recorded for the pristine and shocked samples are displayed in Fig. 1. For the conformation of the crystal structure of the titled crystal, a comparison is made with the standard CIF file (ICSD: 29009) such that the generated XRD pattern of NSH crystal and the obtained XRD pattern of the pristine sample agree well with each other, confirming that the title sample has the $P4_12_12$ space group of the crystal structure.[38] Furthermore, from the XRD patterns of the dynamic shocked samples, as observed in Fig. 1, it is authenticated to be similar to the XRD patterns of the pristine such that it is quite clear that during the shocked conditions, no lattice deformation and crystallographic structural transition are noticed under shocked conditions. Moreover, another possible result of shock wave-induced dehydration has also not taken place so the complete retention of the crystallographic structure could be witnessed, which clearly shows the stable nature of the test sample in its crystallographic configuration under shocked conditions, i.e., for the counts of 50 and 100 shock pulses.

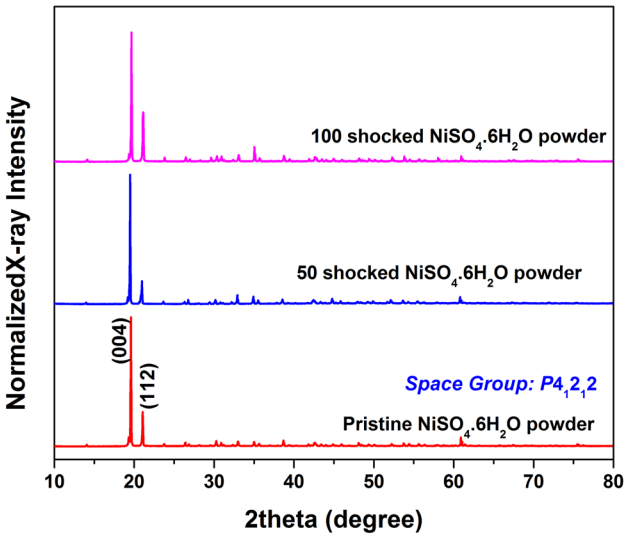

Fig. 1. XRD pattern of the pristine and shocked NSH powder samples.

However, for the single crystal, the test sample undergoes reversible phase transitions of the crystalline to the amorphous for successive shock pulses.[24] For a better understanding of the comparison of the structural stability of the single- and polycrystalline NSH samples, the zoomed-in version of the XRD patterns is shown in Fig. 2. Concerning the polycrystalline samples, a slight change has been observed under 50 and 100 shocked conditions (Fig. 2a). However, as seen in Fig. 2b, the single crystalline NSH crystal has experienced a structural transition occurring between the states of the crystalline and amorphous because of the changes in the parallel and anti-parallel arrangement of the SO_4 units with respect to the growth axis.[24]

Hence, it is worthwhile to obtain a clear understanding of the shock treatment on the title compound. It is quite common for single-crystalline materials to be considered large grain materials with a highly ordered periodic arrangement of the atoms (free of internal grain boundaries), and such materials should have less mechanical stability and structural stability than the polycrystalline samples.[5–8] In the case of polycrystals, the grain and grain boundary densities are much higher than those of the single-crystalline samples, and such grain boundary interfaces have high resistance to external forces such as temperature, pressure, etc., so these materials can withstand the elastic and plastic deformations induced by the external stimuli.[5–8] The present experimental results are in good agreement with the previous reports showing that the single crystal (single grain crystal) has less shock resistance as it undergoes structural phase transitions as well as deformations under shocked conditions. However, the polycrystalline samples have high shock resistance due to the high grain boundary concentration and lower particle sizes. The major reason behind the changes occurring in the structure of the single crystal compared with the polycrystalline sample is that the crystals of lower grain and particle size would ensure the fluctuations (dispersion of shock wave within the materials) during the propagation of shock waves through it, resulting a significant reduction in crystallinity. The actual impact of shock waves and probability of phase transitions and deformations are less for polycrystalline samples compared

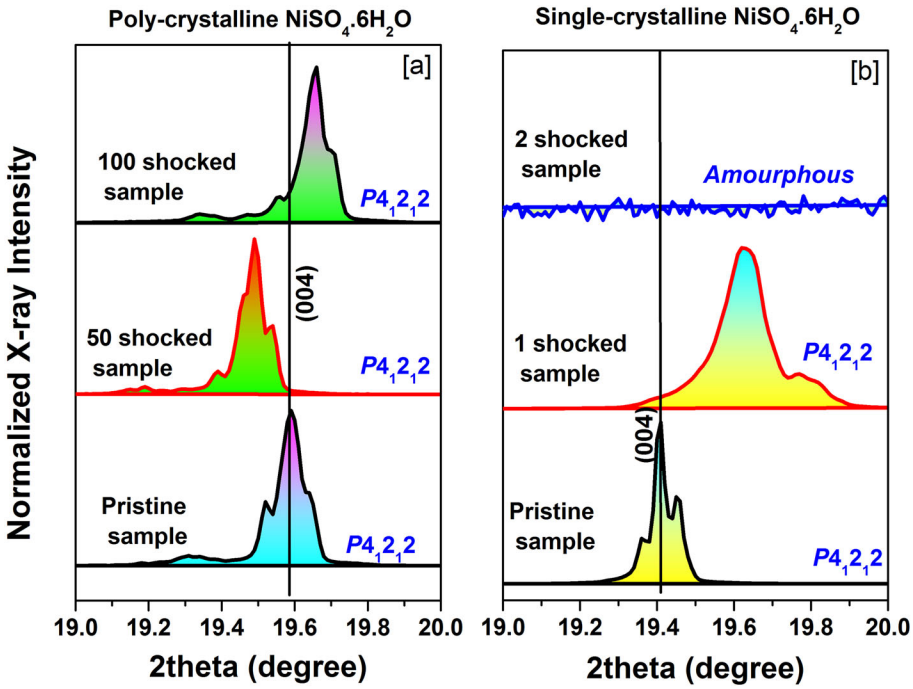

Fig. 2. Zoomed-in versions of the pristine and shocked NSH samples: (a) polycrystalline, (b) single crystalline, with data used from Ref. 24.

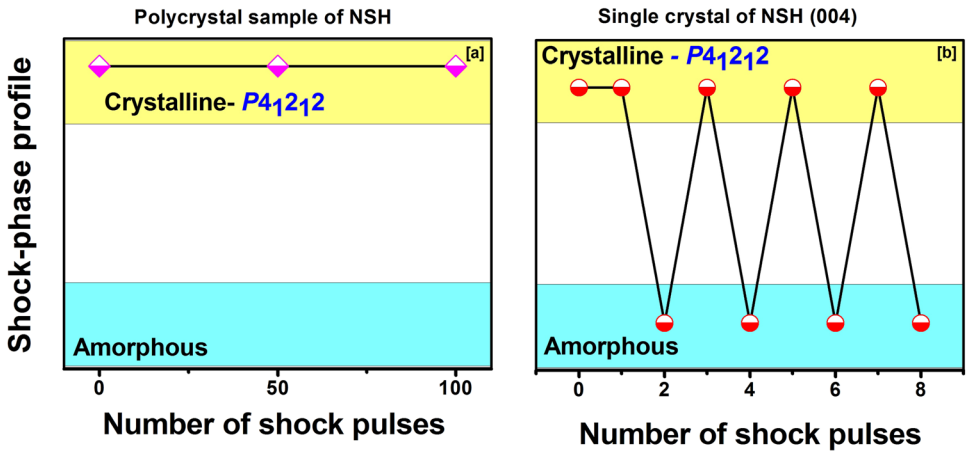

Fig. 3. Shock-phase profiles of NSH crystal: (a) poly-crystal; (b) single-crystal.

to bulk grain materials. Moreover, the polycrystalline materials are composed of many very fine grains, and they also have a linear arrangement, but they are inconsistent in orientation. Thus, the possibility of the occurrence of plastic deformations in the polycrystalline NSH samples is much lower than that of the single crystal of NSH under shocked conditions. Hence, in this aspect also, the shock wave energy is scattered by the grains as well as grain boundary interfaces. Therefore, the net impact of shock waves on the polycrystalline materials is significantly lower than on the single crystals.

Figure 3 shows the shock-phase profile of the single- and polycrystalline materials in accordance with the counts of shock pulses, and based on the observations of the XRD results and phase profiles of the samples, the polycrystalline NSH samples' shock resistance is comparatively higher than for the samples of single-crystalline NSH. Note that the obtained experimental results are in good agreement with the results of several static high-pressure experiments which have been based on the structural stability of the single- and polycrystalline materials,[5,39] and more details are discussed in Raman spectroscopy.

RAMAN SPECTROSCOPY RESULTS

Raman spectrometry has been adopted to assess the phase stability of the polycrystalline samples of NSH in terms of its crystallographic nature, and the obtained Raman profiles are displayed in Fig. 4. For the pristine NSH sample, the characteristic SO_4 Raman bands of υ_2, υ_4, υ_1 and υ_3 appear at 431 cm^{-1}, 462 cm^{-1}, 606 cm^{-1}, 981 cm^{-1} and 1082 cm^{-1}, respectively. Among the four internal Raman bands, υ_2-SO_4 Raman band has a doublet, and the Raman band locations agree well with the literature reports.[40,41] No noteworthy change is noticed in the Raman band such as band shifts (either in lower or higher frequency region) and band shape for the samples under shock-exposed conditions wherein the complete retention of the actual spectra of the title sample against the applied shocks clearly demonstrates that the test samples do not suffer any sort of changes such as crystallographic phase transitions or lattice deformations. Note that it has been well documented in the literature that in the static high-pressure[42] and high-temperature[43] as well as dynamic shocked conditions,[23,44,45] the SO_4 tetrahedral anionic units undergo a significant rotational order-disorder process and induce the crystallographic phase transitions.[42–45] Moreover, in the case of K_2SO_4 single crystal, the most intense Raman band of υ_1-SO_4 is shifted from 984 cm^{-1} to 738 cm^{-1} at the first shocked condition but it comes back to the original position at the second shocked condition because of the reversible phase transition from β-α and α-β K_2SO_4.[23] For Na_2SO_4 single crystal, Raman bands of υ_2, υ_4 and υ_3 show the possible Raman band signatures which undergo changes such as band shift and band appearance/disappearance in accordance with the exposure of shock pulses of various counts due to the crystallographic phase transition of the *F*ddd-Na_2SO_4 (phase-V) to *C*mcm-Na_2SO_4 (phase-III).[44] In addition, for $MgSO_4.7H_2O$ crystal, significant modifications have been noticed in the υ_1-SO_4 Raman band.[45] Mainly for $NiSO_4.6H_2O$ crystal, the symmetric stretching of the υ_1-SO_4 Raman band undergoes a significantly lower frequency shift regarding the number of shocked conditions due to the crystalline to the amorphous phase transitions.[24] Based on the above-discussed Raman spectral changes, it is clearly authenticated that the applied shocked wave transient pressure is high enough to induce crystallographic phase transitions in sulfate cationic materials. However, in the present case, any possible Raman spectral changes could not be observed in the polycrystalline samples even under 50 and 100 shocked conditions.

However, for the $NiSO_4.6H_2O$ sample, the cationic structure of the Ni^{2+} has octahedron coordination with six water molecules. If the applied shock waves could break the water bonds and octahedron coordination network of Ni-$6H_2O$, the υ_1-SO_4 Raman band had to undergo a Raman shift based on the changes (lower hydrates or α-β phase changes). But, surprisingly in the present experiment, no formation of the lower hydrates and crystallographic phase transitions was observed because all the characteristic SO_4 Raman bands remain the same in the position in accordance with the exposure of shock pulses of various counts. The respective position is presented in a plot as shown in Fig. 5.

Ultraviolet Diffused Reflectance Spectroscopy

For colored sulfate anionic crystals such as nickel sulfate hexahydrate[32] and copper sulfate pentahydrate,[46] significant changes can be observed in the electronic spectra while they undergo any of the crystallographic phase transitions or formation of lower hydrates and un-hydrated form of crystals.[36] It is worthwhile to perform the ultra-violet diffused

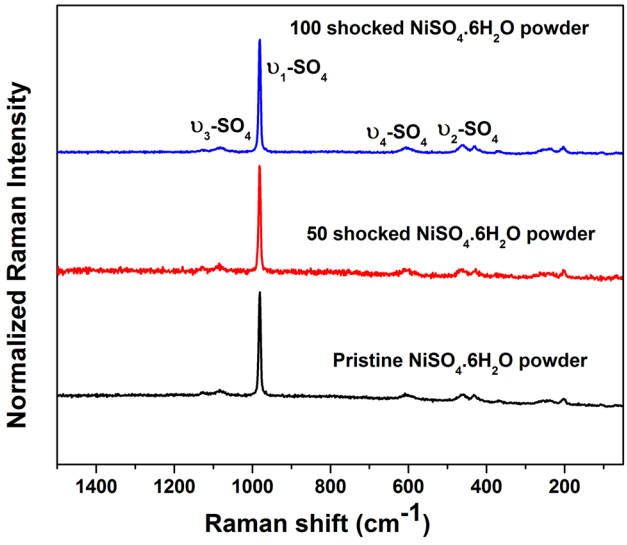

Fig. 4. Raman spectra of the pristine and shocked powder NHS samples.

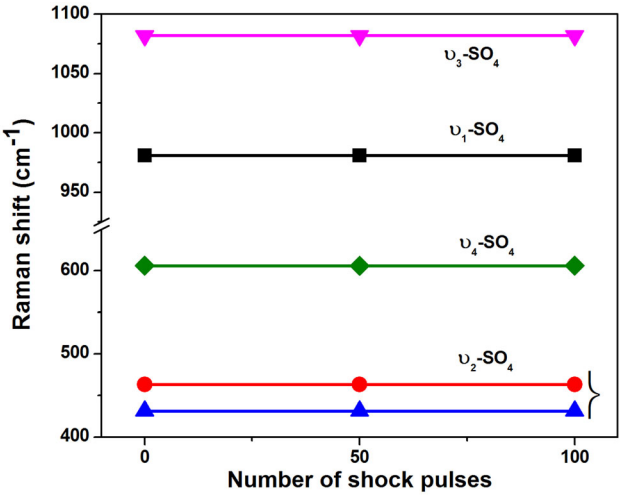

Fig. 5. Raman band positions of the pristine and shocked NSH powder samples.

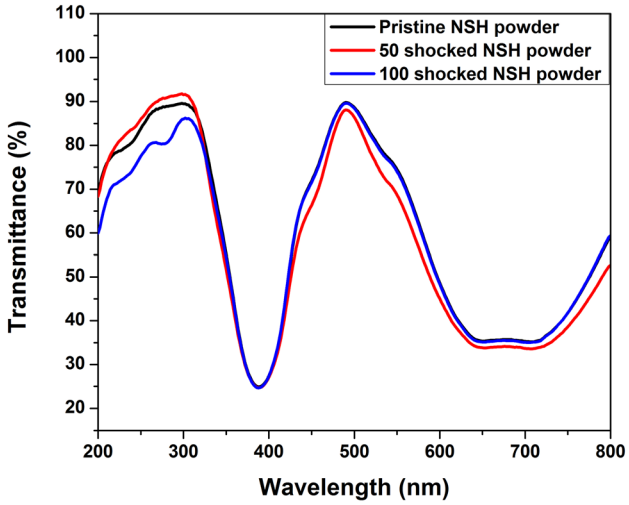

Fig. 6. Optical transmittance spectra of the pristine and shocked NSH powder samples (DRS).

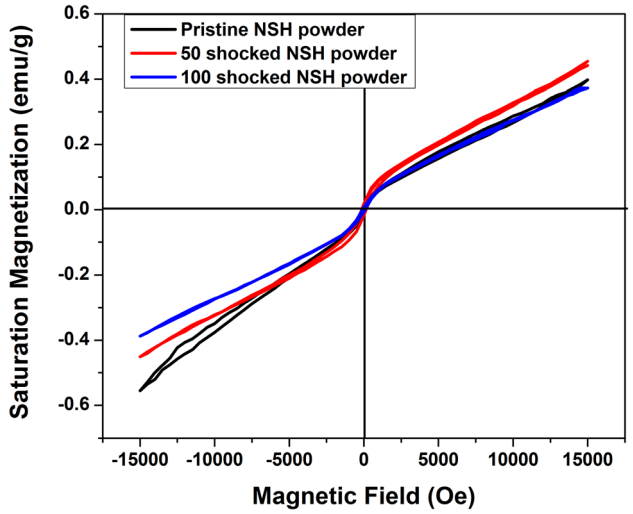

Fig. 7. Magnetic hysteresis loops of the pristine and shocked NSH powder samples.

reflectance spectroscopic study to justify the results of diffraction and Raman spectral analysis in terms of the stability of the crystallographic structure of the titled sample at the exposure of dynamic shocks. The optical transmittance spectra that have been obtained for the pristine as well as shocked samples are portrayed in Fig. 6 for which the spectra have been recorded between the wavelength region of 200 nm and 800 nm.

As reflected in Fig. 6, the transmittance band region of the pristine sample is from 400 nm to 620 nm wherein the pristine sample exhibits the maximum optical transmittance at 490 nm, which is the characteristic electronic spectrum of octahedron coordination of the Ni^{2+} cation.[38] If any shock wave-induced de-hydration process appeared, the transmittance window should have experienced a shift towards the region of higher wavelength as the unhydrated pure $NiSO_4$ is yellow in color.[47] At the shock-exposed conditions, no shift is found in the transmittance window, so the optical transmittance spectra are almost identical for the pristine, 50 and 100 shocked samples. Hence, the quantity of water for the samples remains the same even under shocked conditions, and no signature is seemingly on the cards for the dehydration process influenced by the shock waves. Therefore, based on the analyzed diffraction patterns, vibrational spectra and electronic spectra of the titled crystal under shocked conditions, it could be authenticated that the stability of the crystallographic structure of the title sample is intact under shocked conditions. Furthermore, the titled sample has outstanding crystallographic phase stability in its polycrystalline nature. On the other hand, there is a slight reduction in optical transmittance at the 50-shocked condition, which may be due to the surface defects and particle fragmentation that are also reflected in the XRD results (Fig. 2) of the 50-shocked polycrystalline NSH sample wherein a lower angle shift is noticed compared to the control sample. The lower angle shift of the (004) plane clearly shows the lower degree of crystalline nature compared to the control sample.[21,22] Note that, at the 100-shocked condition, the XRD peak (004) position is similar to the control sample.

Magnetic Properties

The titled compound has to be analyzed for the functional properties while under shocked conditions as it is one of the most required experimental way-outs to make a final call for the overall performance on the relationship between structure-property and stability, and an attempt has been made to investigate the magnetic properties of the samples under shocked conditions. Notably, based on the crystal field theory, different d orbital splitting results (changes in the tetra- and octahedral complexes) in varying numbers of unpaired electrons such that different magnetic behaviors can exist based on the electronic configuration.[48] To assess the magnetic phase of the NSH powder samples, a vibrating sample magnetometer (VSM) has been utilized so the respective magnetic hysteresis loops could be obtained. Figure 7 represents the respective hysteresis loops of the pristine and shocked samples wherein it is witnessed that the pristine sample has a paramagnetic state. Based on the crystal field theory, Ni^{2+} has two unpaired electrons in the 3d orbital and thus no paramagnetism should be present, but the test sample showed weak paramagnetic state which may be due to the inclusion of hydrogen ions or oxygen defects.[48]

In addition, the cationic coordinate network and their shapes would have changed if the water molecules were removed from the Ni^{2+} octahedron,

which could have enforced changes in the number of unpaired electrons. As a result, changes in the magnetic states or degree of the magnetic state might have been observed. As seen in Fig. 7, at the exposure to shocks, no change is observed in the magnetic state regarding the number of shock pulses. Hence, the sample has a high structure-property relationship against the shock wave impulsion. Note that the magnetic state of the nanocrystalline material of α-Fe_2O_3 undergoes changes from the initial magnetic states at the 150-shocked condition [49].

CONCLUSION

Summarizing the present experimental findings, we have initiated the way forward to investigate the crystallographic stability of the polycrystalline NSH samples under dynamic shocked conditions, and the results of the experimental data are drawn from a few analytical techniques such as diffraction, vibrational and electronic spectroscopic techniques. Based on the obtained XRD results, the pristine sample's crystal structure ($P4_12_12$) is retained under shocked conditions, and the Raman spectral results also support the XRD results very well. UV-DRS spectroscopic results clearly demonstrate that the coordination of octahydrate of Ni^{2+} ions remains the same as that of the pristine under shocked conditions. Hence, no de-hydration process has occurred. Moreover, VSM results also make convincing results affirming the stability of the structure-property relationship against the impact of shock waves. The overall experimental results clearly authenticate that the titled polycrystalline samples have higher shock-resistant behavior than the single crystals of NSH. The polycrystalline NSH sample can be a good fit for device fabrications due to its high structural stability under extreme environmental conditions.

SUPPLEMENTARY INFORMATION

The online version contains supplementary material available at https://doi.org/10.1007/s11837-023-06023-x.

ACKNOWLEDGEMENTS

The authors thank Abraham Panampara Research Fellowship and NSF of China (42072055). The project was supported by Researchers Supporting Project number (RSP2023R142), King Saud University, Riyadh, Saudi Arabia. National Research Foundation of Korea (NRF) grant funded by the Korea government (MSIT) (No. 2021R1A4A1032207 and 2022R1C1C1006414).

CONFLICT OF INTEREST

The authors declare that they have no conflict of interest.

REFERENCES

1. Q. Tan, Z. Yan, H. Huang, S. Li, Y. Wang, Y. Feng, X. Zhou, Y. Li, Y. Ren, and S. Antonov, *JOM* 72, 1803 (2020).
2. D. Madapana, H. Ramadas, A.K. Nath, and J.D. Majumdar, *JOM* 75, 109 (2023).
3. W. Cui, M. Yao, D. Liu, Q. Li, R. Liu, B. Zou, T. Cui, and B. Liu, *J. Phys. Chem. B* 116, 2643 (2012).
4. T. Maity, N.K. Gopinath, S. Janardhanraj, K. Biswas, and B. Basu, *Comput Microstruct ACS Appl. Mater. Interfaces* 11, 47491 (2019).
5. M. Hafok, and R. Pippan, *Mater. Sci. Forum* 550, 277 (2007).
6. G. Das, *Cer. Eng. Sci. Proc* 16, 977 (2008).
7. L. Mezeix, and D.J. Green, *Int. J. Appl. Ceram. Technol.* 3, 166 (2006).
8. R. Weber, C.R. Fell, J.R. Dahn, and S. Hy, *J. Electrochem. Soc* 164, 2992 (2017).
9. Y.Q. Zhu, T. Sekine, K.S. Brigatti, S. Firth, R. Tenne, R. Rosentsveig, H.W. Kroto, and D.R.M. Walton, *J. Am. Chem. Soc.* 125, 1329 (2003).
10. V. Jayaram, A. Gupta, and K.P.J. Reddy, *J. Adv. Ceram* 3, 297 (2014).
11. V. Jayaram, and K.P.J. Reddy, *Adv. Mater. Lett.* 7, 100 (2016).
12. S.L. Chinke, I.S. Sandhu, D.R. Saroha, and P.S. Alegaonkar, *ACS Appl. Nano Mater.* 1, 6027 (2018).
13. K. Vasu, H.S.S.R. Matte, S.N. Shirodkar, V. Jayaram, K.P.J. Reddy, U.V. Waghmare, and C.N.R. Rao, *Chem Phys Lett* 582, 105 (2013).
14. S.J. Wang, M.L. Sui, Y.T. Chen, Q.H. Lu, E. Ma, X.Y. Pei, Q.Z. Li, and H.B. Hu, *Sci. Rep* 3, 1086 (2013).
15. Y. Ashkenazy, and R.S. Averback, *Appl. Phys. Lett.* 86, 051907 (2005).
16. S. Zhao, R. Flanagan, E.N. Hahn, B. Kad, B.A. Remington, C.E. Wehrenberg, R. Cauble, K. More, and M.A. Meyers, *Acta Mater.* 158, 206 (2018).
17. Z. Su, W.L. Shaw, Y.-R. Miao, S. You, D.D. Dlott, and K.S. Suslick, *J. Am. Chem. Soc.* 139, 4619 (2017).
18. S. Zhaoa, B. Kada, B.A. Remingtonb, J.C. LaSalviac, C.E. Wehrenbergb, K.D. Behlerc, and M.A. Meyers, *PNAS* 113, 12088 (2016).
19. P. Renganathan, and Y.M. Gupta, *J. Appl. Phys.* 126, 115902 (2019).
20. T.N. Maity, N.K. Gopinath, S. Janardhanraj, K. Biswas, and B. Basu, *ACS Appl. Mater. Interfaces* 11, 47491 (2019).
21. J.H. Joshi, S.A. Martin Britto Dhas, D.K. Kanchan, M.J. Joshi, K.D. Parikh, 31, 14859 (2020).
22. L. Anandaraj, L. Jothi, and J. Mole, *Structure* 1233, 130068 (2021).
23. A. Sivakumar, S. Reena Devi, S. Sahaya Jude Dhas, R. Mohan Kumar, K. Kamala Bharathi, and S.A. Martin Britto Dhas, *Cryst Growth Des.* 20, 7111 (2020).
24. A.Sivakumar, S. Sahaya Jude Dhas, J. Thirupathy, K.P.J. Reddy, R. Suresh Kumar, A.I. Almansour, S. Chakraborty, S.A Martin Britto Dhas, *New J. Chem.* 46, 5091 (2022).
25. M. Kumari, N. Vijayan, D. Nayak, Kiran, P. Vashishtha, A.K. Gangwar, G. Gupta, P.Singh, R.P. Pant, *Opt. Mater.*133, 112986 (2022).
26. A. Sivakumar, A. Saranraj, S. Sahaya Jude Dhas, K. Showrilu, S.A. Martin Britto Dhas, Z. Kristallogr. 236, 1 (2021).
27. A. Sivakumar, S. Sahaya Jude Dhas, S. Balachandar, S.A. Martin Britto Dhas, *J. Elect. Mater.* 48, 7868 (2019).
28. A. Sivakumar, A. Saranraj, S. Sahaya Jude Dhas, P. Sivaprakash, S. Arumugam, S.A. Martin Britto Dhas, *J. Elect. Mater.* 50, 2436 (2021).
29. A. Hazan, G. Hillel, S. Kalabukhov, N. Frage, E.B. Zaretsky, and L. Meshi, *Mater. Charact.* 175, 111061 (2021).

30. A.N. Zhukova, N.S. Sidorovb, A.V. Palnichenkob, V.V. Avdonina, and D.V. Shakhrai, *High. Press. Res* 29, 414 (2009).
31. A. Sivakumar, S. Sahaya Jude Dhas, A.I. Almansour, R. Suresh Kumar, N. Arumugam, K. Perumal, S.A. Martin Britto Dhas, *Solid State. Commun* 340, 114508 (2021).
32. J. Thirupathy, and S.M.S.A. Sahaya Jude DhasJoseMartin Britto Dhas, *Mater Res. Exp.* 6, 086206 (2019).
33. A. Silambarasan, P. Rajesh, and P. Ramasamy, *Spectrochim. Acta Part A* 134, 345 (2015).
34. V.L. Manomenova, E.B. Rudneva, A.É. Voloshin, L.V. Soboleva, A.B. Vasilev, and B.V. Mchedlishvili, *Crystallogr. Rep* 50, 877 (2005).
35. R.R. Choudhury, R. Chitra, I.P. Makarova, V.L. Manomenova, E.B. Rudneva, A.E. Voloshin, and M.V. Koldaeva, *J. Appl. Cryst.* 52, 1371 (2019).
36. M. Friesen, H.M. Burt, and A.G. Mitchell, *Therrnochimica Acta* 41, 167 (1980).
37. A. Sivakumar, S. Balachandar, S.A. Martin Britto Dhas, *Hum Factors Mech. Eng. Def. Saf.* 4, 3 (2020).
38. C.A. Beevers, and H. Lipson, *Z. Kristallogr.* 83, 123 (1932).
39. G. Yang, and S.-J. Park, *A Rev. Mater* 12, 2003 (2019).
40. D. Kiushnamur, *Proc. Ind. Acad Sci* 42, 77 (1955).
41. D. Krishnamurti, *Proc. Ind. Acad Sci.* 47, 355 (1958).
42. T. Sakuntala, A. K. Arora, N.V. Chandra Shekar, P.Ch. Sahu, *Europhys. Lett.*, 44, 728 (1998).
43. F.A.I. El-Kabban, *Phys. Stat. Sol. (A)* 68, 373 (1980).
44. A. Sivakumar, S. Sahaya Jude Dhas, P. Sivaprakash, A.I. Almansour, R. Suresh Kumar, N. Arumugam, S. Arumugam, S.A. Martin Britto Dhas, *New.J. Chem* 45, 16529 (2021).
45. A. Sivakumar, P. Shailaja, S. Sahaya Jude Dhas, P. Sivaprakash, A.I. Almansour, Raju Suresh Kumar, N. Arumugam, S. Arumugam, S. Chakraborty, S.A. Martin Britto ,Dhas, *Cryst. Growth Des.* 21, 5050 (2021).
46. V. Haber, *Chem. Zvesti* 31, 190 (1977).
47. M.J. Nassar, Harrick Scientific Products, Inc, Box 277, Pleasantville, NY 10570.
48. D. Zywitzki, D.H. Taffa, L. Lamkowski, M. Winter, D. Rogalla, M. Wark, A. Devi, *Inorg. Chem.* 59, 10059 (2020).